Available online at www.sciencedirect.com
SCIENCE DIRECT®
ELSEVIER
Journal of Nuclear Materials 343 (2005) 247–252
journal of nuclear materials
www.elsevier.com/locate/jnucmat

Charpy impact tests on martensitic/ferritic steels after irradiation in SINQ target-3

Yong Dai [a,*], Pierre Marmy [b]

[a] *Spallation Neutron Source Division, Paul Scherrer Institut, 5252 Villigen PSI, Switzerland*
[b] *Fusion Technology Materials, CRPP/EPFL, 5232 Villigen PSI, Switzerland*

Abstract

Charpy impact tests were performed on martensitic/ferritic (MF) steels T91, F82H, Optifer-V and Optimax-A/-C irradiated in SINQ Target-3 up to 7.5 dpa and 500 appm He in a temperature range of 120–195 °C. Results demonstrate that for all the four kinds of steels, the ductile-to-brittle transition temperature (DBTT) increases with irradiation dose. The difference in the DBTT shifts (ΔDBTT) of the different steels is not significant after irradiation in the SINQ target. The ΔDBTT data from the previous small punch ($\Delta\ DBTT_{SP}$) and the present Charpy impact ($\Delta DBTT_{CVN}$) tests can be correlated with the expression: $\Delta\ DBTT_{SP} = 0.4\Delta DBTT_{CVN}$. All the ΔDBTT data fall into a linear band when they are plotted versus helium concentration. The results indicate that helium effects on the embrittlement of MF steels are significant, particularly at higher concentrations. It suggests that MF steels may not be very suitable for applications at low temperatures in spallation irradiation environments where helium production is high.

1. Introduction

Martensitic/ferritic (MF) steels were selected for liquid metal containers in high-power spallation targets because of their higher mechanical strength at ⩽500 °C, better thermal mechanical properties and lower irradiation induced swelling as compared to annealed austenitic steels [1,2]. However, it is known that MF steels suffer from irradiation induced embrittlement in the low temperature regime, <350 °C. Moreover, a number of studies demonstrated that the embrittlement could be enhanced greatly by the helium (He) content in MF steels produced via nuclear reactions between neutrons and nuclides such as ^{10}B and ^{59}Ni [3–5]. Since the He production rate in steels under the irradiation in spallation targets is very high, to understand the behaviours of MF steels in such irradiation environments is an important materials issue for developing high-power liquid metal spallation targets, particularly for those to be operated at temperatures below 350 °C. Hence, a number of MF steels were included in the SINQ target irradiation program (STIP) and irradiated to doses up to 20 dpa [6,7]. Some interesting results have been obtained. For example, investigations on the microstructure of MF steels, 9Cr1MoVNb (T91) and F82H, show that high-density helium bubbles of about 1 nm large can be already observed in samples irradiated to about 10 dpa and 500 appm He at about 200 °C and the bubble size increases with irradiation temperature and dose [8]. In the present paper, the Charpy impact tests have been performed on MF steels, T91, F82H,

* Corresponding author. Tel.: +41 56 310 4171; fax: +41 56 310 4529.
E-mail address: yong.dai@psi.ch (Y. Dai).

0022-3115/$ - see front matter © 2005 Elsevier B.V. All rights reserved.
doi:10.1016/j.jnucmat.2004.12.020

Optifer-V, Optimax-A and -C irradiated in SINQ Target-3 to a maximum dose of 7.5 dpa in a temperature range of 120–195 °C.

2. Experimental

2.1. Materials and specimen

The materials studied in this work include the conventional MF steel T91, and the reduced activation MF steels F82H, Optifer-V, Optimax-A and Optimax-C obtained from the fusion materials program. The T91 steel was obtained from Oak Ridge National Laboratory (ORNL). It was in form of a 10 mm thick plate with heat treatments as such: normalized at 1040 °C for 1 h in air and followed by air cooling; then tempered at 760 °C for 1 h followed by air cooling. The F82H (8Cr–2W, the IEA Heat 9741) steel was obtained from the fusion materials program. The steel was normalized at 1040 °C for 38 min and followed by air cooling; then tempered at 750 °C for 1 h followed by air cooling. The Optifer-V (9Cr–1W) steel was developed at Forschungszentrum Karlsruhe (FZK). It was in form of a forged bar with a cross-section of about 24 mm × 24 mm. The specimens were provided by Forschungszentrum Jülich (FZJ). The Optimax-A (9Cr–1W) and -C (9Cr–2W) steels were developed by the Fusion Technology Materials, CRPP/EPFL, Switzerland. The steels were in form of 8–10 mm thick plates with heat treatments: normalized at 1050 °C for 1 h followed by air cooling, then tempered at 750 °C for 2 h followed by air cooling. The compositions of the steels are listed in Table 1.

One-third-size Charpy specimens measuring 3.3 × 3.3 × 25.4 mm with 0.51 mm-deep 30° V-notches were used.

2.2. Irradiation

The specimens were irradiated in the first SINQ target irradiation program (STIP-I) at the Paul Scherrer Institut (PSI), Switzerland during 1998 and 1999. For each of the steels, the specimens were irradiated to two doses in a range of 4.2–7.5 dpa. The information of the irradiation dose, helium and hydrogen concentrations and irradiation temperature of the specimens are given in Table 2. The details of STIP-I can be found in Ref. [6] and the information about the determination of irradiation dose, helium and hydrogen concentrations can be found in Ref. [9]. As can be seen in Table 2, the ratio of He/dpa is not constant due to the different proton and neutron spectra at different positions in the target.

2.3. Mechanical tests and TEM observation

Charpy impact tests were performed using an instrumented Charpy impact testing machine with an energy capacity of 30 J. The machine was equipped with a temperature control device (TCD) which can vary the testing temperature from about −180 to 500 °C. A test at higher or lower temperature than room temperature started in 15 min after inserting the specimen into the TCD which had reached the desired temperature already. The time from transporting the specimen from the TCD till to breaking the specimen was less than 2 s. During this time the temperature had almost no change. The force–time curves and the absorbed energy were automatically measured.

3. Results

The results of the T91 steel are shown in Fig. 1. For unirradiated samples, the upper-shelf energy (USE) is about 9.4 J and the ductile-to-brittle transition temperature (DBTT) is about −54 °C, which is defined as the temperature corresponding to the half of the USE. After irradiation to 4.6 dpa and 265 appm He at about 120 °C, the USE of the samples decreases to 5.8 J and, meanwhile, the DBTT increases to about 54 °C, which gives a DBTT shift of about 108 °C. The other group of samples irradiated to higher dose of 6.8 dpa and 450 appm He at 180 °C shows no more reduction in USE but a further increase in DBTT to 165 °C.

The F82H samples were irradiated at the same conditions as the T91 samples, namely one group irradiated to 4.6 dpa and 265 appm He at about 120 °C, and the other group irradiated to 6.8 dpa and 450 appm He at 180 °C. The unirradiated F82H samples show a higher USE of

Table 1
Compositions of the MF steels

Steel	Fe	Cr	Ni	Mo	Mn	V	Nb	W	Ta	C	Si	N	P
T91	Balance	8.32	0.09	0.86	0.48	0.20	0.06			0.01	0.15	0.055	0.01
F82H	Balance	7.87	0.02		0.1	0.19		1.98	0.03	0.09	0.07	0.007	0.003
Optifer-V	Balance	9.48	0.06		0.55	0.24		0.98	0.065	0.12	0.04	0.044	0.0015
Optimax-A	Balance	9.3	<0.01	0.09	0.60	0.24	<0.01	0.97		0.098	0.02	0.001	0.01
Optimax-C	Balance	9.5	<0.01	0.15	0.40	0.25	<0.01	1.97		0.11	0.03	0.007	0.011

Table 2
Irradiation conditions and Charpy test results of F82H, T91, Optifer-V and Optimax-A and -C samples

Materials	Specimen ID	dpa	He (appm)	He/dpa ratio (appm/dpa)	H[a] (appm)	Irrd. temp. (°C)	DBTT (°C)	ΔDBTT (°C)	USE (J)
T91	Un-irr	–	–	–	140	–	−54	–	9.4
	I-A	4.6	266	57.8	560	122	54	108	5.8
	I-B	6.8	449	66	800	185	165	219	5.8
F82H	Un-irr	–	–	–	140	–	−84	–	10.5
	P-A	4.6	266	57.8	560	122	50	134	9.0
	P-B	6.8	449	66	800	185	71	155	8.4
Optifer-V	Un-irr	–	–	–	140	–	−112	–	10.1
	M-A	5.0	285	57	610	130	−27	139	10
	M-B	7.5	500	66.7	880	195	70	182	6.0
Optimax-A	Un-irr	–	–	–	140	–	−80	–	10.5
	N-A	4.2	250	59.5	520	115	−7	73	9.5
Optimax-C	Un-irr[b]	–	–	–	140	–	−55	–	10.5
	N-B	6.15	405	65.9	730	175	57	112	9.3

[a] The hydrogen contents are calculated based on the measured results [9]. The values for unirradiated samples are referred to that of unirradiated F82H [10].
[b] Data of unirradiated Optimax-C were provided by Baluc [11].

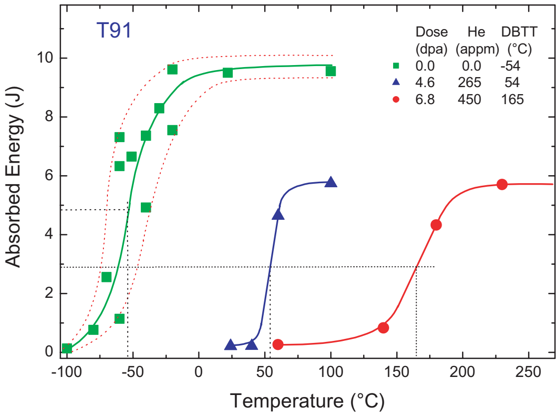

Fig. 1. The testing temperature dependence of the absorbed energy of the T91 Charpy samples at different irradiation doses.

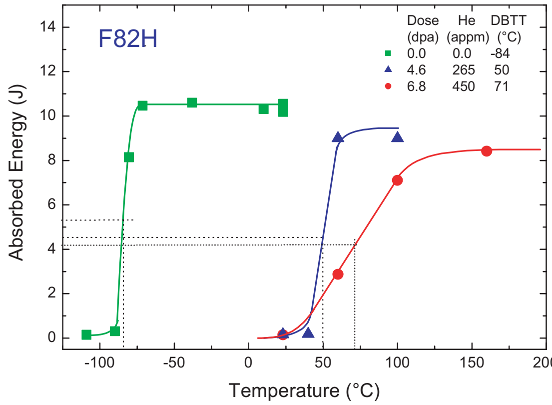

Fig. 2. The testing temperature dependence of the absorbed energy of the F82H Charpy samples at different irradiation doses.

10.5 J and lower DBTT of −84 °C, as compared to the unirradiated T91 samples. After irradiation to 4.6 dpa and 265 appm He, the USE of the F82H samples decreases slightly to 9.0 J but the DBTT increases substantially to 50 °C. At the higher dose of 6.8 dpa and 450 appm He, the USE decreases to 8.4 J and the DBTT rises to 71 °C, as shown in Fig. 2.

Fig. 3 presents the results of the Optifer-V samples. In unirradiated condition, the USE is about 10 J and the DBTT is at about −112 °C. After irradiation to 5.0 dpa and 285 appm He at 130 °C, the USE remains unexpectedly unchanged although the DBTT shifts up to −27 °C. However, the samples irradiated to 7.5 dpa and 500 appm He at 195 °C present a lower USE of about 6 J and a DBTT of 70 °C.

The unirradiated Optimax-A samples have similar USE and DBTT values like the unirradiated F82H samples, namely about 10.5 J and −80 °C and also show a very sharp ductile to brittle transition, as can be seen in Fig. 4. Although the unirradiated Optimax-C samples were not available for testing in the present work, it is shown by Baluc [11] that its USE is similar to that of the unirradiated Optimax-A, while its DBTT is −55 °C. After irradiation to 4.2 dpa and 250 appm He at 115 °C, the USE and DBTT of the Optimax-A samples change to 9.5 J and −7 °C, respectively. The Optimax-C samples which were irradiated to 6.2 dpa and 405 appm He at 175 °C show an USE of 9.3 J and a DBTT of 57 °C.

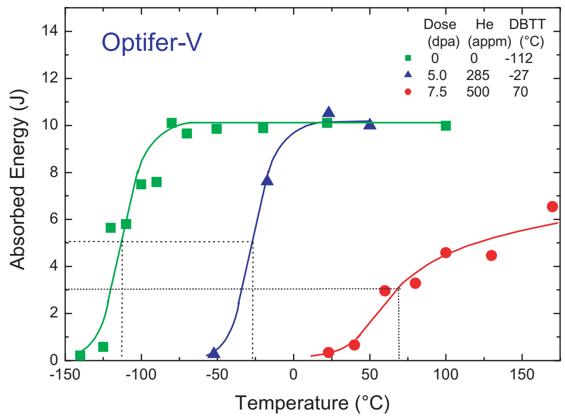

Fig. 3. The testing temperature dependence of the absorbed energy of the Optifer-V Charpy samples at different irradiation doses.

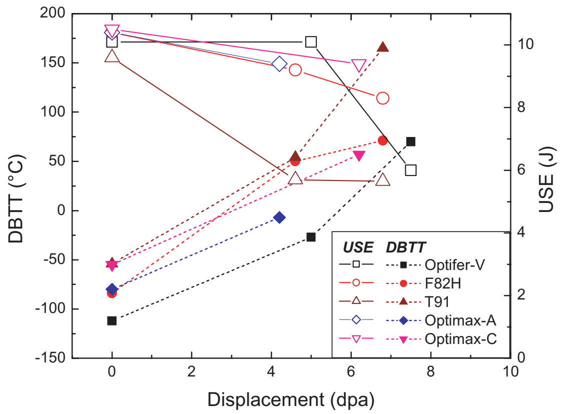

Fig. 5. The dose dependence of the DBTT and USE for the T91, F82H, Optifer-V, Optimax-A and -C after irradiation.

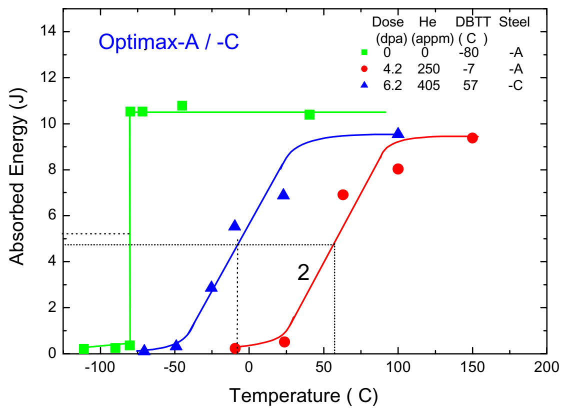

Fig. 4. The testing temperature dependence of the absorbed energy of the Optimax-A/-C Charpy samples at different irradiation doses.

The USE and DBTT values of all the samples are listed in Table 2 and also plotted as a function of irradiation dose in Fig. 5. It is interesting to note that for all the four steels, the DBTT increases with increasing irradiation dose and does not saturate in the dose range.

4. Discussion

The irradiation in SINQ targets differs greatly from irradiations in nuclear reactors in respect to the high production rate of helium, hydrogen and other transmutation elements through spallation reactions. Therefore, the irradiation effects in materials in spallation targets cannot be simply simulated by any other methods such as neutron irradiations and ion implantations. The different characteristics of irradiations in nuclear reactors and spallation targets demonstrate significant different results. For example, in the STIP irradiation, high-density tiny He bubbles were observed in F82H and T91 samples irradiated to 5.8 dpa at about 200 °C [8], while no bubbles or voids could be observed in T91 and HT9 samples irradiated to 38 dpa at 300 °C in the HFIR [12].

For MF steels, one of the most concerned issues is helium induced embrittlement effects at low temperatures. It is well accepted that the irradiation induced DBTT shift is mainly attributed to the irradiation induced hardening [13,14], which is often expressed as $\Delta DBTT \propto \Delta\sigma_y$ ($\Delta\sigma_y$ is the increase of yield stress). However, it is also noted that helium can play an important role in the DBTT shift after irradiation. The early data of the T91 and HT9 irradiated in the FFTF and the HFIR indicated that the irradiation in the HFIR introduced a much larger ΔDBTT than in the FFTF. The reason was believed to be due to the higher helium concentration produced in the samples irradiated in the HFIR [15,16]. More recently, some experiments in the HFR at Petten [5,17] demonstrated that the difference in the DBTT shift of different MF steels after irradiation could be attributed to the different helium production in those steels. Furthermore, the saturation of the DBTT shift with irradiation dose followed more or less the profile of the transformation of helium from boron via the $B(n,\alpha)$ Li reaction. Either our previous results of small punch tests [18,19] or the present results of Charpy impact tests indicate that the DBTT of the MF steels increases with irradiation dose and even quicker at higher doses above about 6 dpa. This is inconsistent with the behaviour observed after neutron irradiations where the DBTT shift saturates at a dose of 1–5 dpa. The continuous increase of DBTT at higher doses is believed to be due to helium effects. Our previous small-punch tests demonstrated that the DBTT shifts of different steels were linearly proportional to helium concentration [19]. In fact, the DBTT shift evaluated from the small punch tests ($\Delta DBTT_{SP}$) can be well correlated with what obtained from the present Charpy impact tests with the expression: $\Delta DBTT_{SP} = 0.4\Delta DBTT_{CVN}$. Fig. 6 includes the results from both the small punch and Charpy impact tests of the samples from the same irradiation. It illustrates that all the data fall into a linear band against helium concentration.

Furthermore, the large difference in the DBTT shift of different MF steels after irradiation in the HFR [5,17] is not observed in the present case. This can be understood based on the helium effects, because the helium production rates in the different MF steels are very close during irradiation in the SINQ target.

Although it is not understood yet why the DBTT shifts of the MF steels depend linearly on helium concentration, it is clear that helium has significant effects on the embrittlement of MF steels in the low temperature regime. This suggests that MF steels are not very suitable for applications at low temperatures in spallation irradiation environments where helium production is high.

It is also well known that hydrogen has embrittlement effects on MF steels at low temperatures. As illustrated in Table 2, the hydrogen concentrations in the present Charpy samples are in a range of 500–900 appm. While the three SP samples of T91, F82H and Optimax-A showing the highest DBTT shift in Fig. 6 have only about 300–400 appm hydrogen, which is not much higher than that in unirradiated samples. Therefore, one cannot correlate the DBTT shift with the hydrogen content. This implies that hydrogen might not be very effective on the DBTT shift in the present case, although it cannot be excluded. Nevertheless, further investigations will be performed to clarify the hydrogen effects in STIP samples.

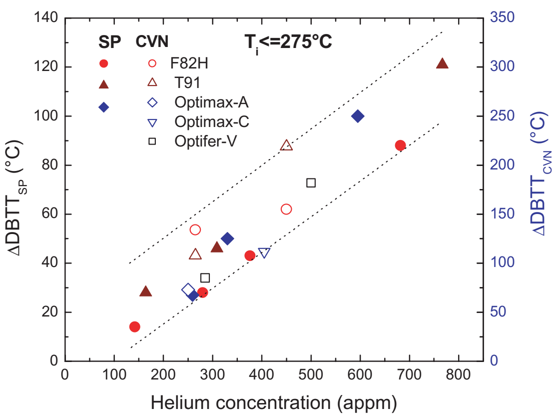

Fig. 6. DBTT shift as a function of helium concentration for both the previous small punch tests [17] and the present Charpy tests.

For other elements such as phosphorus and sulphur, it is believed that their productions in the present dose range are still too low (<50 appm) to induce a significant DBTT shift.

5. Conclusions

Charpy impact tests have been conducted on the MF steels T91, F82H, Optifer-V and Optimax-A and -C irradiated in SINQ Target-3 up to 7.5 dpa in a temperature range of 120–195 °C. Results demonstrate that:

1. For all the four kinds of steels, the DBTT increases with irradiation dose. The difference in the DBTT shifts of the different steels is not significant after irradiation in the SINQ target.
2. ΔDBTT data from the previous small punch tests and the present Charpy impact tests can be correlated with the expression: $\Delta DBTT_{SP} = 0.4\Delta DBTT_{CVN}$. All the ΔDBTT data fall into a linear band when they are plotted versus helium concentration.
3. The results indicate that helium effects on the embrittlement of MF steels are significant, particularly at higher concentration levels. It suggests that martensitic steels are not very suitable for applications at low temperatures in spallation irradiation environments where helium production is high.

Acknowledgments

The authors would like to thank Mr R. Thermer for his help on the reparation of experiments. Drs K. Farrell (ORNL), F. Carsughi (FZJ) and M. Victoria (CRPP/EPFL) are acknowledged for providing specimens of T91, Optifer-V and Optimax-A and -C steels.

This work is included in the SPIRE (Irradiation effects in martensitic steels under neutron and proton mixed spectrum) subprogram of the European 5th Framework Program and supported by the Swiss Bundesamt für Bildung und Wissenschaft.

References

[1] Y. Dai, in: Proceedings of ICANS-XIII and ESS-PM4, 11–19 October 1995, PSI, p. 604.
[2] R.L. Klueh, in: Proceedings of First International Workshop on Spallation Materials Technology, 23–25 April 1996 Oak Ridge, p. 3.3.
[3] R.L. Klueh, J.M. Vitek, W.R. Corwin, D.J. Alexander, J. Nucl. Mater. 155–157 (1988) 973.
[4] R.L. Kluch, D.J. Alexander, J. Nucl. Mater. 187 (1992) 60.

[5] E.I. Materna-Morris, M. Rieth, K. Ehrlich, in: Effects of Radiation on Materials: 19th Internatinal Symposium (ASTM STP 1366, 2000), p. 597.
[6] Y. Dai, G.S. Bauer, J. Nucl. Mater. 296 (2001) 43.
[7] Y. Dai, X. Jia, R. Thermer, F. Groeschel, EU FP5 SPIRE program Deliverable no. 47, or PSI Technical Report TM-34-04-08.
[8] X. Jia, Y. Dai, J. Nucl. Mater. 318 (2003) 207.
[9] Y. Dai, Y. Foucher, M. James, B. Oliver, J. Nucl. Mater. 318 (2003) 167.
[10] P. Marmy, B. Oliver, J. Nucl. Mater. 318 (2003) 132.
[11] N. Baluc, submitted for publication.
[12] P.J. Maziasz, R.L. Klueh, J.M. Vitek, J. Nucl. Mater. 141–143 (1986) 929.
[13] A. Kimura, M. Narui, T. Misawa, H. Matsui, A. Kohyama, J. Nucl. Mater. 258–263 (1998) 1340.
[14] R.L. Klueh, D.R. Harries, High-Chromium Ferritic and Martensitic Steels for Nuclear Applications, ASTM stock number: MONO3, printed in USA, 2001, Chapter 14.
[15] J.M. Vitek, W.R. Corwin, R.L. Klueh, J.R. Hawthorne, J. Nucl. Mater. 141–143 (1986) 948.
[16] R.L. Klueh, D.J. Alexander, J. Nucl. Mater. 179–181 (1991) 733.
[17] M. Rieth, B. Dafferner, H.D. Roehrig, J. Nucl. Mater. 258–263 (1998) 1147.
[18] Y. Dai, X. Jia, K. Farrell, J. Nucl. Mater. 318 (2003) 192.
[19] X. Jia, Y. Dai, J. Nucl. Mater. 323 (2003) 360.